JB
Journals.ASM.org

Chemosensory Regulation of a HEAT-Repeat Protein Couples Aggregation and Sporulation in *Myxococcus xanthus*

Cynthia L. Darnell,[a] Janet M. Wilson,[b] Nitija Tiwari,[c] Ernesto J. Fuentes,[c] John R. Kirby[a]

Department of Microbiology, University of Iowa, Iowa City, Iowa, USA[a]; Division of Select Agents and Toxins, Office of Public Health Preparedness and Response, Centers for Disease Control and Prevention, Atlanta, Georgia, USA[b]; Department of Biochemistry, University of Iowa, Iowa City, Iowa, USA[c]

Chemosensory systems are complex, highly modified two-component systems (TCS) used by bacteria to control various biological functions ranging from motility to sporulation. Chemosensory systems and TCS both modulate phosphorelays comprised of histidine kinases and response regulators, some of which are single-domain response regulators (SD-RRs) such as CheY. In this study, we have identified and characterized the Che7 chemosensory system of *Myxococcus xanthus*, a common soil bacterium which displays multicellular development in response to stress. Both genetic and biochemical analyses indicate that the Che7 system regulates development via a direct interaction between the SD-RR CheY7 and a HEAT repeat domain-containing protein, Cpc7. Phosphorylation of the SD-RR affects the interaction with its target, and residues within the α4-β5-α5 fold of the REC domain govern this interaction. The identification of the Cpc7 interaction with CheY7 extends the diversity of known targets for SD-RRs in biological systems.

Chemosensory systems are complex, highly modified variations of two-component systems (TCS) used to control bacterial behavior. While the canonical chemosensory system regulates flagellum-based motility (1, 2), it has become clear that these systems can also regulate alternative cellular functions (ACFs) (3). Several examples are known in which ACF systems affect multicellular development, including biofilm (4–7), cyst (8), and fruiting-body (9, 10) formation. Like systems that regulate chemotaxis (1, 2), chemosensory systems are composed of a core phosphorelay (defined by the presence of a CheA homolog and its cognate response regulator partner) and an associated adaptation module conferring sensitivity to gradients in the environment.

For chemosensory systems, stimuli are perceived by methyl-accepting chemotaxis proteins (MCPs), and the signal is transmitted via CheW coupling proteins to a CheA kinase. CheA autophosphorylates on a conserved His residue and subsequently passes the phosphoryl group to a conserved Asp residue within a receiver (REC) domain of a response regulator (RR) to control the output of the system. The domain organization of the RR can vary. For prototypical TCS, ~85% of REC domains are covalently linked to DNA binding domains (DBD), whereas many REC domains encoded within chemosensory systems exist as single domain response regulators (SD-RR), including CheY. During chemotaxis, *Escherichia coli* CheY interacts directly with the flagellar components FliM and FliN to bias the rotation of the flagella, thereby regulating behavior (11–13). The CheY-FliM/N affinity is dependent on the phosphorylation state of CheY (14).

Despite the extensive knowledge gained through many studies on *E. coli* CheY, there are few examples of the roles and targets of SD-RRs for ACF systems. The search for those roles and targets is complicated by the fact that the *E. coli* chemotaxis system contains a second response regulator, CheB, responsible for demethylation of the MCPs to bring about adaptation in the presence of a stimulus. However, in the case of CheB, the REC domain is covalently linked to a methylesterase domain that becomes activated upon phosphorylation of the REC domain. Additionally, CheY~P interacts with CheZ, which promotes dephosphorylation of the response regulator to reset the system. Thus, two REC domains with very similar topologies interact with multiple, distinct targets, including the CheA histidine kinase, the flagellar switch complex, a methylesterase, and a phosphatase. Similarly, SD-RRs are likely to have a large array of potential interaction partners for the regulation of alternative cellular functions.

The soil bacterium *Myxococcus xanthus* has over 40 SD-RRs, 6 of which are genetically associated with chemosensory systems (15, 16). *M. xanthus* is a model organism for the study of signal transduction and development. Cells coordinate their movement to mount predatory attacks (17). When cells sense low nutrient availability, they begin a developmental program that results in multicellular fruiting-body formation and differentiation into resistant myxospores (18). Regulation of these complex processes is governed in part by a large repertoire of signaling proteins, including 127 TCS and 8 chemosensory systems (15, 16). In this report, we characterize the Che7 ACF chemosensory system for its role in *M. xanthus* development. We identify the immediate output for the SD-RR CheY7 to be a HEAT repeat domain-containing protein, Cpc7, required for the appropriate coupling of aggregation and sporulation by *M. xanthus*.

MATERIALS AND METHODS

Strains and growth conditions. Wild-type *M. xanthus* DZ2 was used in this study. Bacterial strains and plasmids are listed in Table S1 in the supplemental material. *M. xanthus* was grown routinely in Casitone-yeast extract (CYE) media at 32°C (19). Kanamycin and spectinomycin were used at 100 μg/ml and 800 μg/ml, respectively. *E. coli* strains were grown in Luria broth (LB) at 37°C. Kanamycin (40 μg/ml), spectinomycin

Received 27 May 2014 Accepted 18 June 2014
Published ahead of print 23 June 2014
Address correspondence to John R. Kirby, john-kirby@uiowa.edu.
Supplemental material for this article may be found at http://dx.doi.org/10.1128/JB.01866-14.

doi:10.1128/JB.01866-14

(100 μg/ml), and ampicillin (100 μg/ml) were used for maintenance of plasmids.

DNA manipulations and strain construction. Standard cloning procedures were used. Primers are listed in Table S2 in the supplemental material. Site-directed mutagenesis was performed using the QuikChange site-directed mutagenesis kit (Agilent), and constructs were verified by sequencing (Nevada Genomics).

In-frame deletions were made in *M. xanthus* using counterselection plasmid pBJ114 as previously reported (20). Briefly, 1-kb flanking regions were PCR amplified and cloned into pBJ114 using restriction enzymes. Plasmids were electroporated into *M. xanthus* and transformants plated in soft agar (0.7%) containing 40 μg/ml of kanamycin. Resulting merodiploid colonies were grown for several generations and plated on CTT (1% Casitone, 10 mM morpholinepropanesulfonic acid [MOPS; pH 7.6], 1 mM KH_2PO_4) media containing 2% galactose for counterselection. Galactose-resistant, kanamycin-sensitive colonies were screened by colony PCR for deletions using gene-specific primers.

Complementation constructs were integrated at the Mx8 site using standard protocols (21). Plasmids were electroporated into *M. xanthus* and transformants plated in soft agar containing 40 μg/ml of kanamycin. Resulting colonies were grown for several generations, and integration was verified by site-specific PCR.

Developmental assays. Strains were grown to mid-log phase and harvested by centrifugation (8,000 × *g*). Cells were washed in deionized water (dH_2O) and concentrated to 8×10^8 cells/ml (see Fig. 2A, 4, and 5; see also Fig. S2 and S3 in the supplemental material) or 2×10^8 cells/ml (see Fig. 2B). Ten-microliter spots were plated on CFL agar [10 mM MOPS (pH 7.6), 1 mM KH_2PO_4, 8 mM $MgSO_4$, 0.02% $(NH_4)_2SO_4$, 0.02% citrate, 0.02% pyruvate, and 15 mg/liter of Casitone] (22) and incubated at 32°C. Pictures were taken using a Nikon Eclipse 50i phase-contrast microscope and a Nikon SMZ1500 dissecting microscope with a Q Imaging MicroPublisher 5.0 RTV camera and software. For spore counts, 10 spots were inoculated per plate. At various time points, cells were scraped using a razor blade and resuspended in 1 ml of dH_2O. Samples were incubated at 55°C and sonicated using Branson sonifier 150 set at intensity 4 for 10 s to kill vegetative cells. Dilutions were plated on CYE media in soft agar, and CFU were counted.

Protein purification. CheY7, CheY7^{D53A}, CheY7^{F107A}, and Cpc7 were cloned into pET28a expression vector to generate a T7-6× His N-terminal tag. For acetyl phosphate (AcP) experiments, proteins were purified by standard batch procedure as previously described (23). For fluorescence binding assays, proteins were affinity purified over a Ni^{2+} column and a size exclusion column. For all proteins, purity was determined by Coomassie staining.

Acetyl phosphate labeling. Proteins were radiolabeled with acetyl phosphate ([^{32}P]AcP) as described previously (10, 24). Briefly, [^{32}P]AcP was generated using *E. coli* acetate kinase (Sigma). Protein was removed by centrifugation in an Amicon Ultra filter unit (Millipore). A 5 μM concentration of CheY7 or CheY7^{D53A} was incubated with AcP for 1 h and cleaned over a Zeba spin desalting column (Thermo Scientific). Samples were separated by SDS-PAGE and visualized using a phosphor screen and Typhoon imager (GE).

Bacterial two-hybrid analysis. Fusion proteins were generated in pUT18c and pKT25 plasmids (see Table S2 in the supplemental material for primers). Reporter strain BTH101 was transformed and colonies grown in LB overnight at 30°C. Samples were resuspended in Z buffer, sonicated (intensity 4 for 10 s), and centrifuged to remove debris (16,000 × *g*). One hundred microliters of lysate was assayed in a standard Miller assay. Protein concentrations were determined by Bradford assay (Bio-Rad).

Fluorescence binding assay. Intrinsic tryptophan fluorescence was measured at 25°C using a Fluorolog 3 spectrofluorimeter (Jobin Yvon, Horiba) in a 1.5-ml sample of 0.5 μM Cpc7 in Tris buffer (25 mM Tris-HCl [pH 7.6], 125 mM NaCl, 5% glycerol). For each measurement, excitation was at 291 nm (14.7-nm slit width). The fluorescence emission spectrum was collected in the range of 300 to 400 nm (14.7-nm slit width). CheY7 or CheY7^{F107A} was titrated to a final concentration of 15 μM. Each titration point was stirred for 30 s. Peak fluorescence was normalized to a buffer control titration. The K_d (dissociation constant) for each titration was determined by fitting buffer-corrected data to the following equation by nonlinear regression (Sigma Plot; SPPS, Inc.), where A is fluorescence at each step during the titration, A_{min} is the initial fluorescence, B_{max} is maximum fluorescence at saturation, and $[RR]$ is the total concentration of response regulator in solution.

$$(A - A_{min}) = \frac{B_{max}[RR]}{K_d + [RR]}$$

The resulting dissociation constant was the average of three independent experiments.

Circular dichroism. CheY7 and CheY7^{F107A} proteins were purified as described for the fluorescence binding assay. Samples were diluted to a final concentration of 20 μM in Tris buffer (25 mM Tris-HCl [pH 7.6], 125 mM NaCl, 5% glycerol) and analyzed using a 1-mm cuvette in a Jasco J-815 circular-dichroism (CD) spectrometer.

RESULTS

Identification of the *che7* cluster. *M. xanthus* encodes eight chemosensory systems, four of which have been described in some detail: Frz (25–27), Dif (28, 29), Che3 (9, 10), and Che4 (30). The central processing component for all chemosensory systems is CheA. In previous work, we analyzed the *M. xanthus* genome for *cheA* homologs and identified four additional clusters, including Che5 to -8 (31, 32). Because each cluster contains unique genes predicted to encode novel protein functionality regarding inputs and/or outputs, we further characterized the Che7 system (genes *MXAN_6965 to MXAN_ 6957*) for its role in development in *M. xanthus*. One unique component encoded within the *che7* cluster is a HEAT repeat domain-containing protein, Cpc7. This protein has homology to phycocyanobilin lyases found in cyanobacteria. As determined by reverse transcription-PCR (RT-PCR), the Che7 cluster encodes CheY7, CheA7, CheW7, Mcp7, Cpc7, CheB7, CheR7, and Des7 (Fig. 1; see also Fig. S1 in the supplemental material).

An *in silico* analysis of Che7-like systems based on *cheA7*, *mcp7*, and *cpc7* sequences revealed loci with the same gene order. A phylogenetic tree was produced based on a CheA-CheR-CheB concatenated protein, as described previously (33) (Fig. 1B). Notably, *che7* was found largely within two clades, the myxobacteria and cyanobacteria. Within the myxobacteria, *che7* was found only in species with a developmental cycle: *Myxococcus fulvus*, *Corallococcus coralloides*, *Stigmatella aurantiaca*, and *Sorangium cellulosum*. In contrast, *che7* was not found in the closely related species *Anaeromyxobacter dehalogens*, a myxobacterium that does not undergo development, or within other members of the *Deltaproteobacteria* clade. Importantly, each *che7* cluster contains a *cpc7* homolog. Together, these results suggest that Che7 may regulate a process specific to myxobacteria capable of development and that Cpc7 may be involved in regulation of that process.

Cyanobacteria that possess a *che7*-like locus, including a Cpc7-like HEAT repeat gene annotated as a phycocyanobilin lyase, include *Arthrospira* species, *Crinalium episammum*, and *Oscillartoria acuminata* (15). Phycocyanobilin lyase homologs have been described and have roles in maintenance of light-harvesting phycobilisomes (34, 35). Thus, it is not surprising to find these genes in cyanobacteria. However, HEAT repeat proteins can mediate protein-protein interactions (36), bind iron (37), stabilize [Fe-S] clusters (38, 39), and interact with chemotaxis proteins (40). In

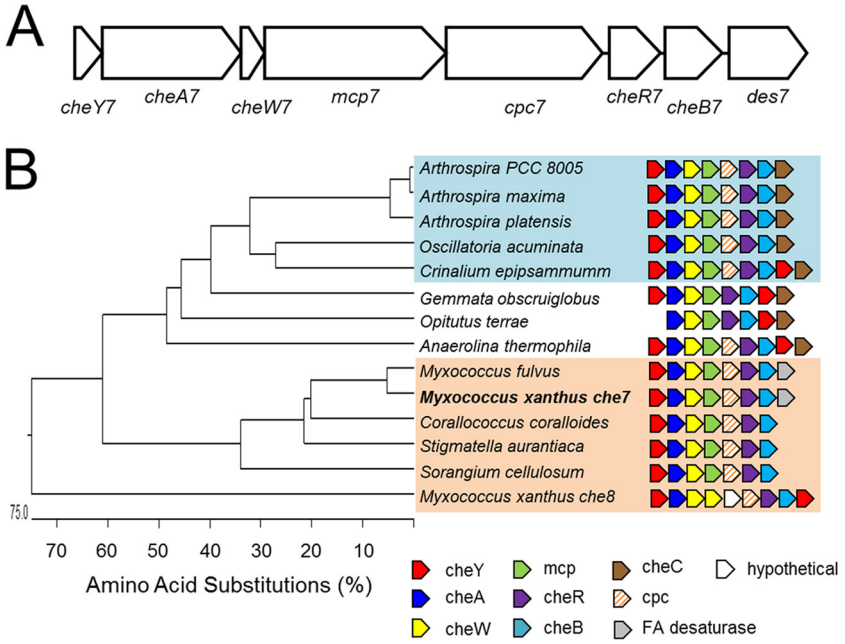

FIG 1 The *M. xanthus che7* locus and phyletic tree of *che7* clusters. (A) The *che7* cluster contains six chemosensory genes (*cheY7*, *cheA7*, *cheW7*, *mcp7*, *cheR7*, and *cheB7*) as well as accessory genes *cpc7* (HEAT repeat protein) and *des7* (fatty acid [FA] desaturase). (B) Shown is a phylogenetic tree based on CheA-CheR-CheB concatenated proteins from cyanobacterial and myxobacterial species that possess Cpc homologs (see the text). Gene order for the corresponding clusters is shown at right. Blue shaded boxes indicate cyanobacterial species containing *che7*. Orange shaded boxes indicate myxobacteria containing *che7*. *cpc7* is conserved in most *che7* clusters, whereas *des7* is specific to *Myxococcus* species.

addition to cyanobacteria, *che7* loci were found in *Gemmata obscuriglobus*, *Opitutus terrae*, and *Anaerolinea thermophila*. Based on the occurrence of the *cpc7* gene in chemosensory clusters (Fig. 1B), Che7 may have originated in cyanobacteria with a role in harvesting light, whereas in myxobacteria the system appears to have evolved to regulate some aspect of development (see below).

Mutations in the Che7 system alter aggregation and development into spores. To determine the role of Che7 during the *M. xanthus* life cycle, we constructed in-frame deletions in genes within the *che7* cluster. We did not observe any defects in growth, motility, or exopolysaccharide (EPS) production during vegetative growth (see Fig. S1 in the supplemental material; other data not shown). Because the *che7* system is found in developing myxobacteria, we tested each strain for development on CFL starvation media. We found that *che7* mutants had severe aggregation defects relative to the parent strain, DZ2 (Fig. 2A). For example, the Δ*cheY7* mutant cells formed poorly defined aggregates that never matured into discrete fruiting bodies. Cells sporulated nonetheless, both within mounds and between the aggregates as individual cells; this is in contrast to the wild type, which sporulates almost exclusively within fruiting bodies (Fig. 2). Despite aberrant sporulation by the Δ*cheY7* mutant, motile rods could be found at the periphery of the colony (see Fig. S2B in the supplemental material), indicating that sporulation occurs only in a subset of cells,

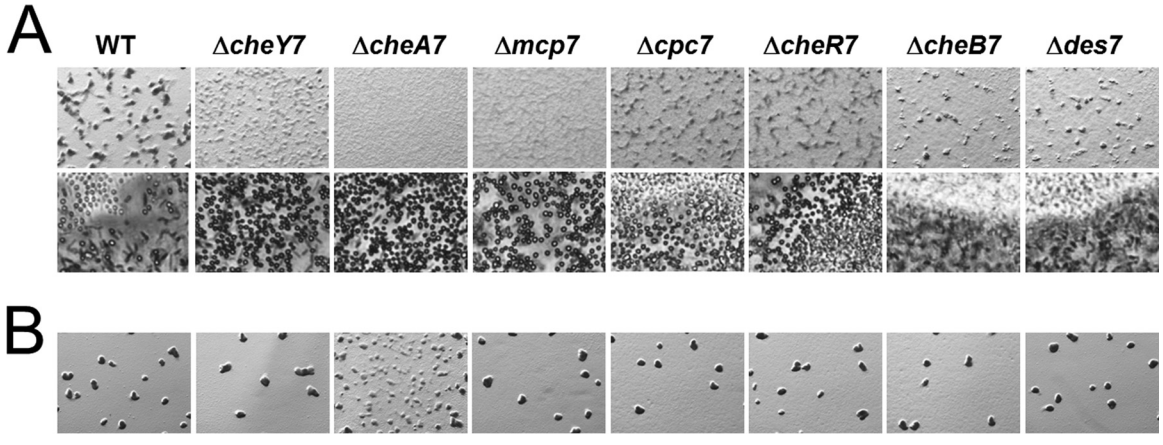

FIG 2 *che7* mutant cells display decoupled aggregation and sporulation during development. Strains were plated on CFL starvation agar at concentrations of 8×10^8 cells/ml (A) and 2×10^8 cells/ml (B). Images were taken at 72 h at magnifications of ×30 (A, top row) and ×200 (A, bottom row) and at 120 h at a magnification of ×30 (B). Development is characterized by cells aggregating to form fruiting bodies. Light-refractile spores can be seen within the aggregates.

TABLE 1 Viable spore count

Genotype	Viable sport count, CFU (mean ± SD)		
	Day 3	Day 4	Day 5
WT[a]	$(1.50 \pm 1.93) \times 10^3$	$(2.23 \pm 0.46) \times 10^6$	$(1.44 \pm 0.59) \times 10^7$
Δ*cheA7*	$(2.13 \pm 0.31) \times 10^5$	$(3.63 \pm 0.15) \times 10^6$	$(1.20 \pm 0.61) \times 10^7$
Δ*cheY7*	$(2.20 \pm 1.14) \times 10^5$	$(5.00 \pm 1.67) \times 10^6$	$(6.84 \pm 8.06) \times 10^6$
Δ*cpc7*	$(8.03 \pm 2.89) \times 10^4$	$(2.57 \pm 1.70) \times 10^6$	$(8.63 \pm 10.00) \times 10^6$

[a] WT, wild type.

similar to findings for the wild type. Strains with mutations in *cpc7* and *cheR7* also aggregated poorly compared to the wild type. The Δ*cheA7* and the Δ*mcp7* mutants further decoupled aggregation from sporulation, forming lawns of spores at the initial spot of inoculation. The Δ*cheB7* and Δ*des7* mutant cells formed normal fruiting bodies, although the timing of aggregation was delayed compared to that for the parent.

To determine if the Δ*che7* mutant spores were viable, we harvested cells over time, sonicated and heat killed vegetative cells, and plated resistant spores for CFU determination. The results for the parent, Δ*cheY7*, Δ*cheA7*, and Δ*cpc7* strains are shown in Table 1. At 72 h, we saw an increase of 2 orders of magnitude in the *che7* strains relative to the parent. However, by 120 h, the parent and the *che7* mutants had reached similar CFU. Therefore, while *che7* strains sporulate earlier than the parent and outside aggregates, ultimately the same number of cells sporulate as observed for the parent. We also assessed sporulation efficiency for the remaining *che7* mutants at 72 h and found that sporulation levels were inversely correlated with aggregation (Fig. 2; see also Table S3 in the supplemental material) such that early sporulation relative to the parent occurred without aggregation. Together, the data suggest that Che7 is involved in coupling aggregation to sporulation.

M. xanthus development depends on cell density (41). We tested if density played a role for the phenotypes described above by lowering the concentration of cells plated (Fig. 2B). At the lower cell density, we saw that the *che7* mutants formed fruiting bodies indistinguishable from those of the parent, with the exception of the Δ*cheA7* strain. The Δ*cheA7* strain formed immature aggregates, indicating a partial rescue. Therefore, *che7* mutant strains are capable of developing normally under certain conditions, and high cell density is tied to Che7 coordination of aggregation and sporulation.

CheY7 functions as a single domain response regulator. Based on homology to *E. coli* CheY, we predicted that *M. xanthus* CheY7 is the RR for the Che7 system. As an SD-RR, CheY7 would likely interact with other protein(s) to generate a response to the signal sensed by the Che7 system. Therefore, we studied CheY7 in more detail. An alignment between *M. xanthus* CheY7 and *E. coli* CheY revealed that the residues required for phosphorylation and substrate binding are present in the *M. xanthus* homolog (Fig. 3A) (42–44). Furthermore, the predicted $(\beta\text{-}\alpha)_5$ structure appeared to be conserved when modeled using Phyre2 to thread CheY7 onto *Vibrio cholerae* CheY3 (Fig. 3A and B) (45).

We first complemented the Δ*cheY7* mutant using an epitope-tagged version of *cheY7* under the control of the *M. xanthus pilA* promoter, which is known to constitutively drive gene expression when cells are plated on agar (46). The construct was integrated at the Mx8 phage attachment site in both the parent and Δ*cheY7*

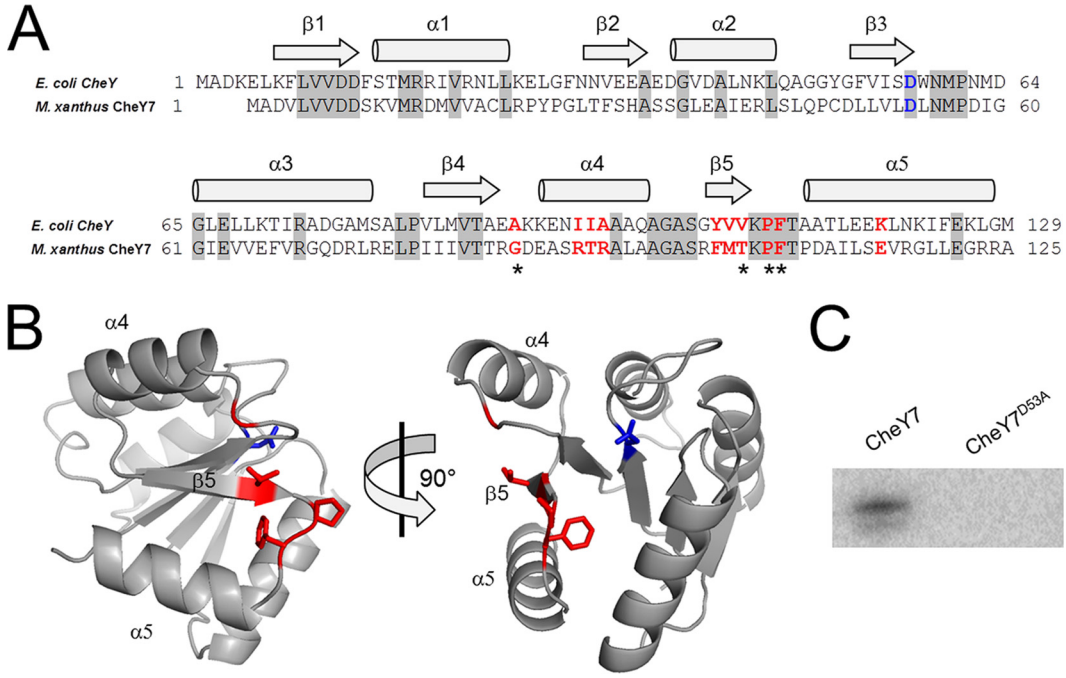

FIG 3 CheY7 is a phosphorylatable SD-RR. (A) Amino acid alignment of *E. coli* CheY and *M. xanthus* CheY7. Residues important for interaction between *E. coli* CheY7 and FliM/CheZ substrates are indicated in red. The conserved aspartate residue that is the site of phosphorylation in REC domains is highlighted in blue. Gray shading indicates identity between *E. coli* and *M. xanthus* homologs. Regions of the proteins predicted to encode alpha helices or beta sheets are indicated above the alignment. (B) Depiction of two views of *M. xanthus* CheY7 threaded onto *V. cholerae* CheY3. Residues affecting CheY7-Cpc7 interactions as determined in the bacterial two-hybrid assay (Table 2) are shown in red. The putative site of phosphorylation is shown in blue. (C) *In vitro* phosphorylation of CheY7 and $CheY7^{D53A}$ using acetyl phosphate (see Materials and Methods) is shown. The D53A mutation eliminates phosphorylation of CheY7.

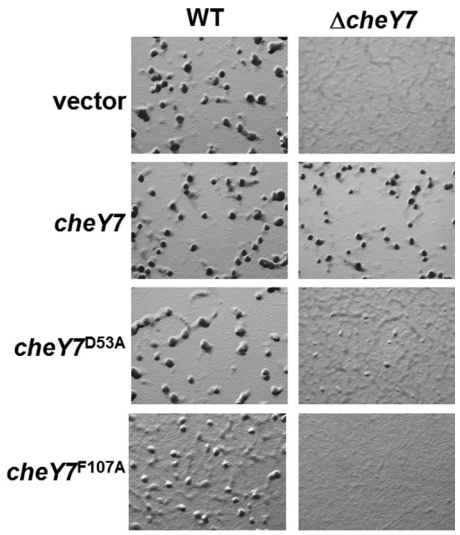

FIG 4 *In vivo* analysis of developmental defects for *cheY7* mutants. *cheY7* mutant alleles predicted to affect phosphorylation (D53A) or interaction with downstream targets (F107A) were assayed for defects in development. Cells were plated on CFL starvation agar and assessed for aggregation. Each allele is under the control of a constitutive *pilA* promoter and was integrated at the Mx8 phage attachment site. The vector control represents an insertion at the ectopic locus without a corresponding *cheY* allele.

strains (21). Expression of a second copy of *cheY7* in the parent strain did not have any apparent impact on fruiting-body formation (Fig. 4). Expression of tagged *cheY7* was sufficient to restore wild-type aggregation and sporulation within fruiting bodies in the Δ*cheY7* mutant (Fig. 4).

Response regulators are typically phosphorylated on a conserved Asp residue. CheY7 contains an Asp at position 53, as well as other residues known to be important for phosphorylation (Fig. 3A) (42–44). To test if the conserved Asp53 was important for cellular function, we changed the residue to Ala. We integrated the tagged alleles at the Mx8 site and assayed for the ability to complement the Δ*cheY7* strain (Fig. 4). Importantly, CheY7^{D53A} was unable to complement the aggregation phenotype, suggesting that phosphorylation of CheY7 is important under these conditions. We also generated a CheY7^{D53E} construct to mimic the activated state of CheY7. However, we found that the D53E variant was unable to complement the Δ*cheY7* strain under conditions tested (data not shown), indicating that CheY7^{D53E} is a null allele similar to CheY7^{D53A}.

To further support a role for phosphorylation of Asp53, we determined if CheY7 could be phosphorylated *in vitro* by the high-energy phosphodonor acetyl phosphate (AcP), a technique used routinely for phosphorylating response regulators (47). We purified the wild-type and D53A versions of CheY7 using affinity purification. We then generated radiolabeled AcP using purified *E. coli* acetate kinase (Sigma). Incubation of wild-type CheY7 with AcP yielded a radiolabeled band when separated by SDS-PAGE (Fig. 3C). Thus, CheY7 can be phosphorylated *in vitro*. In contrast, the D53A construct did not yield a phosphorylated product, indicating the requirement of Asp53 for phosphorylation. Together, the *in vivo* and *in vitro* data support a role for CheY7 as a bona fide phosphorylatable SD-RR that is modified at the conserved position typically found in REC domains.

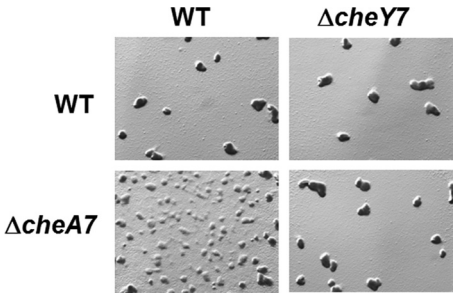

FIG 5 Epistasis analysis of Δ*cheA7* and Δ*cheY7* strains. Strains were plated on CFL agar at a concentration of 2×10^8 cells/ml. Images were taken at ×30 at 120 h. The data indicate that CheY7 is the downstream target for CheA7.

CheY7 interacts with and functions downstream of CheA7. We sought to identify a kinase that modulates the CheY7 phosphorylation state *in vivo*. Based on the paradigm for chemotaxis, we predicted that CheY7 would function downstream of CheA7. To determine this, we performed epistasis analysis between mutations resulting in deletions for *cheY7* and *cheA7*. At low cell density, a phenotypic difference between the Δ*cheY7* and Δ*cheA7* strains is clear: Δ*cheA7* cells are defective at aggregation, and Δ*cheY7* cells appear more similar to the parent strain (Fig. 2B). To determine if CheY7 is downstream of CheA7, we constructed a Δ*cheY7* Δ*cheA7* double mutant strain and assayed for development at low cell density (Fig. 5). Consistent with the predicted model, the Δ*cheY7* Δ*cheA7* strain phenocopied the Δ*cheY7* parent, indicating that the Δ*cheY7* mutation is epistatic to the Δ*cheA7* mutation. These data support a model in which CheY7 is the cognate RR for CheA7.

To test if the interaction between CheA7 and CheY7 was direct, we conducted further studies. Cognate kinases and response regulators interact to transfer phosphoryl groups. We attempted to purify CheA7 from *E. coli* but were unable to produce stable, soluble protein for *in vitro* phosphorylation assays. In lieu of direct phosphotransfer assays, we assessed if CheA7 and CheY7 could interact using the *Bordetella* bacterial two-hybrid system, in which interacting proteins couple two halves of adenylate cyclase (T18 and T25) to drive a LacZ reporter (Table 2) (48). Expression of T18-CheY7 and T25-CheA7 in the *E. coli* BTH101 reporter strain resulted in an ~60-fold increase in β-galactosidase activity compared to the vector controls. Based on these data, CheA7 and CheY7 interact *in vivo*. Together with the epistasis analysis, these data lead us to conclude that CheA7 and CheY7 comprise the core signaling pathway for the Che7 system in *M. xanthus*.

Complementation of CheY7 requires Cpc7. Based on studies from other ACF chemosensory systems, we predicted that either the Cpc7 or Des7 proteins would act as an output for the Che7 system and possibly interact directly with CheY7. To test if either Cpc7 or Des7 functions downstream of CheY7, we employed epistasis analyses based on the differential phenotypes displayed during development (as shown in Fig. 2A). To do so, we constructed additional mutant strains (Δ*cheY7* Δ*des7* and Δ*cheY7* Δ*cpc7*) and assayed them for their capacity to sporulate outside aggregation centers or fruiting bodies. Comparison with the Δ*cheY7* and Δ*des7* mutant strains and the Δ*cheY7* Δ*des7* strain revealed that the double mutant phenocopied the Δ*cheY7* parent strain, indicating that CheY7 functions downstream of Des7 or that Des7 is not directly part of the Che7 pathway (Fig. 6, top row). In contrast, the Δ*cheY7*

TABLE 2 Results of bacterial two-hybrid analysis

Protein coupled to plasmid		β-Galactosidase activity/μg of protein (mean ± SD)	% of WT
pUT18c	pKT25		
		0.53 ± 0.05	
CheY7		0.43 ± 0.09	
	CheA7	0.54 ± 0.05	
CheY7	CheA7	29.93 ± 1.82	100.0
	Cpc7	0.65 ± 0.08	
CheY7	Cpc7	15.21 ± 1.01	100.0
D53A	Cpc7	5.26 ± 3.17	34.6
D53E	Cpc7	7.40 ± 2.49	48.7
G86A	Cpc7	4.25 ± 0.11	28.0
R91A	Cpc7	13.35 ± 1.86	87.8
T92A	Cpc7	17.23 ± 4.81	113.3
R93A	Cpc7	10.65 ± 1.94	70.0
F102A	Cpc7	13.19 ± 1.82	86.7
M103A	Cpc7	12.74 ± 1.77	83.8
T104A	Cpc7	5.73 ± 3.75	37.7
P106A	Cpc7	0.65 ± 0.25	4.3
F107A	Cpc7	0.87 ± 0.64	5.7
E115A	Cpc7	8.12 ± 0.66	53.4

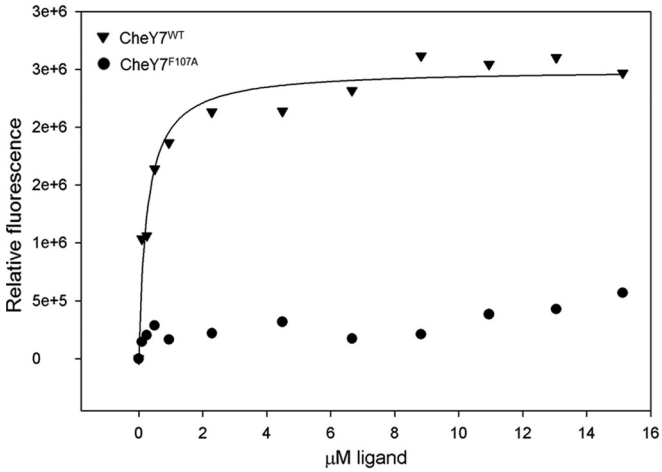

FIG 7 Intrinsic tryptophan fluorescence assay for binding affinity between Cpc7 and CheY7. The fluorescence spectrum for purified epitope-tagged Cpc7 (0.5 μM) was obtained (see Materials and Methods). CheY7^{WT} (▼) or CheY7^{F107A} (●) was titrated in and spectra were normalized to a buffer control. The change in fluorescence is reported as relative fluorescence over the concentration of ligand. The fitted curve for CheY7^{WT} was calculated using nonlinear regression to reveal a K_d of 0.30 ± 0.05 μM. Each titration was done in triplicate and a representative experiment is presented.

Δ*cpc7* strain was able to aggregate poorly, resembling the Δ*cpc7* strain rather than the Δ*cheY7* strain (Fig. 2A and 6). This result suggests that Cpc7 likely acts downstream of CheY7.

The results shown in Fig. 4 demonstrate that the Δ*cheY7* mutant could be complemented with the wild-type allele of *cheY7*. Based on the phenotypes of the double mutant strains listed above, we predicted that expressing *cheY7* from an ectopic locus would result in complementation of the Δ*cheY7* Δ*des7* mutant but not the Δ*cheY7* Δ*cpc7* mutant. Developmental assays revealed that the Δ*cheY7* Δ*des7* strain was complemented for its ability to aggregate and sporulate, indicating that CheY7 does not require Des7 for function during starvation-induced development (Fig. 6, bottom row). In contrast, expression of CheY7 was unable to complement the Δ*cheY7* Δ*cpc7* strain. In fact, addition of CheY7 resulted in an exaggerated phenotype with very poor aggregation and a corresponding lawn of spores. A possible explanation for the difference in aggregation between the Δ*cheY7* Δ*cpc7* strain and the Δ*cheY7* Δ*cpc7* strain expressing *cheY7* could be cross talk due to removal of a CheY7 target. Alternatively, CheY7 could have an additional unidentified target. Nonetheless, the data indicate that CheY7 requires Cpc7 to coordinate aggregation and sporulation in *M. xanthus*.

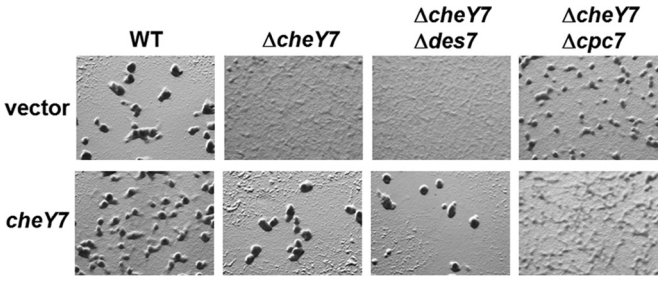

FIG 6 Epistasis analysis of Δ*cheY7*, Δ*des7*, and Δ*cpc7* strains. *cheY7* was expressed from the Mx8 phage attachment site (see text) in various mutant backgrounds and assayed for defects in development. Cells were plated on CFL starvation agar and assessed for aggregation. The *cpc7* mutation is epistatic to the mutation in *cheY7* and could not be complemented by expression of *cheY7* in the absence of *cpc7*.

CheY7 interacts with Cpc7. Response regulators have been shown to interact with a variety of other domains to control the output of both two-component and chemosensory systems. Since CheY7 requires Cpc7 to complement the aggregation and sporulation phenotypes associated with Δ*cheY7* mutant cells, we hypothesized that CheY7 and Cpc7 interact directly. To test this possibility, we used the bacterial two-hybrid system to determine if an interaction occurs between CheY7 and Cpc7. When expressed in the reporter BTH101, the T18-CheY7 and T25-Cpc7 fusion products produced an ~30-fold increase in β-galactosidase reporter activity over that of the vector-based controls, indicating a relatively strong protein-protein interaction, similar to that shown for CheA7 and CheY7 (Table 2). We also generated a T18-CheY7^{D53A} fusion construct to determine if phosphorylation was important for this interaction. Interestingly, the D53A version of CheY7 was able to promote binding; however, the allele did not result in wild-type levels of activity (Table 2). These results are consistent with *E. coli* CheY and CheY~P both displaying the capacity to interact with FliM, though the latter has a higher affinity (14, 49, 50). Therefore, it is likely that phosphorylation of CheY7 enhances binding with Cpc7 *in vivo*.

As a further verification of the CheY7-Cpc7 interaction, we designed an *in vitro* assay. We purified tagged versions of wild-type CheY7 and Cpc7 using affinity and size exclusion chromatography. Using the intrinsic fluorescence of the three tryptophan residues in Cpc7 (W48, W296, and W531), we measured the fluorescence spectrum as a function of CheY7 concentration. Titration of Cpc7 with CheY7 produced a change in fluorescence (Fig. 7) corresponding to an apparent K_d of 0.30 ± 0.05 μM, indicating that a relatively tight interaction occurs *in vitro*. On the basis of the *in vivo* bacterial two-hybrid results, the epistasis analyses, and the *in vitro* fluorescence binding data, we conclude that CheY7 and Cpc7 make a direct interaction to promote development in *M.*

xanthus. Moreover, we have identified an interacting partner for SD-RR or CheY-like proteins not previously described.

The α4-β5-α5 region of CheY7 is required for interaction with Cpc7. *E. coli* CheY interacts with both FliM and CheZ via its C-terminal α4-β5-α5 fold (43, 49–51). To assess whether the same region of CheY7 is required for interaction with Cpc7, we performed site-directed mutagenesis on residues known to affect the *E. coli* CheY-FliM and CheY-CheZ interactions (see residues in red in Fig. 3A). Based on that alignment and using site-directed mutagenesis, we generated mutations corresponding to alanine substitutions in the following residues in *M. xanthus* CheY7: G86, R91, T92, R93, F102, M103, T104, P106, F107, and E115. Each mutant allele was cloned into the bacterial two-hybrid system and assayed for interaction with Cpc7. While some alleles retained wild-type levels of reporter activity when expressed with the Cpc7 fusion, several displayed reduced activity, including G86A, T104A, P106A, and F107A (Table 2). The mutation corresponding to P106A likely affects secondary structure, whereas G86, T104, and F107 may be required for maintaining contacts with Cpc7. Of note is residue F107, as it is conserved in both *E. coli* and *M. xanthus* CheY homologs. The F107A mutant was severely reduced for reporter activity, suggesting a prominent role for interaction with the target Cpc7.

To further evaluate the interaction between Cpc7 and CheY7, we purified the tagged-CheY7^{F107A} variant and tested it using the tryptophan fluorescence binding assay. Indeed, the mutant CheY7 protein was unable to alter the fluorescence profile of Cpc7 (Fig. 7). To determine if the F107A mutant protein was properly folded, we generated circular dichroism spectra for CheY7^{F107A} and wild-type CheY7. Both proteins maintained secondary structures consistent with proper folding (see Fig. S3 in the supplemental material). Lastly, we assayed the CheY7^{F107A} protein for its effect on development. We expressed the tagged CheY7^{F107A} in the parent and the Δ*cheY7* mutant. CheY7^{F107A} was unable to complement the Δ*cheY7* mutant (Fig. 4). In addition, expression of CheY7^{F107A} in the wild-type background reduced the ability of cells to aggregate properly, indicating partial dominance in *trans* over the wild-type CheY7 protein. One possible explanation is that the F107A variant is phosphorylated *in vivo*, titrating phosphoryl groups from wild-type CheY7, but cannot interact with the Cpc7 target to regulate development. From these results, we conclude that the C-terminal α4-β5-α5 region of CheY7 is required for its interaction with Cpc7 to regulate fruiting-body formation in *M. xanthus*. Additionally, as described for other REC-protein interactions, we conclude that the conserved C-terminal α4-β5-α5 fold governs interactions between SD-RRs and their targets.

DISCUSSION

In this report, we describe a protein-protein interaction between an SD-RR (CheY7) and a HEAT repeat protein (Cpc7) required for the proper regulation of development in *M. xanthus*. Due to the structural and functional diversity of domains known to interact with REC domains, it has been difficult to identify targets for SD-RR regulation. The identification of the Cpc7 interaction with CheY7 extends the diversity of known targets for SD-RRs in nature. Nevertheless, the requirements for SD-RR (or REC) interaction with a given target appear to be conserved: phosphorylation of the SD-RR affects interaction with its target and the α4-β5-α5 fold within the REC domain governs the interaction. Phosphorylation of CheY7 at position D53 is required to complement a

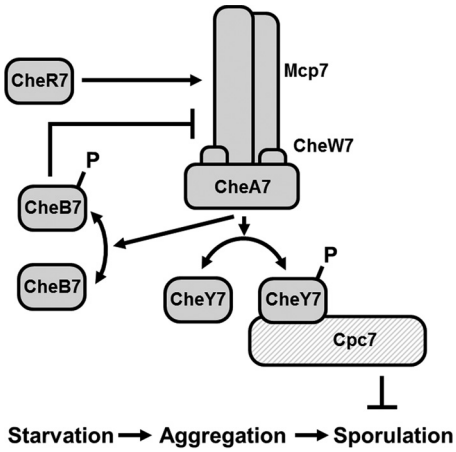

FIG 8 Model for Che7 regulation of development. *M. xanthus* responds to starvation stress by aggregating into fruiting bodies. Subsequently, a subpopulation of cells convert to resistant spores. Che7 regulates the phosphorylation state of CheY7 via the CheA7 histidine kinase. CheY7∼P interacts with HEAT repeat protein Cpc7 to inhibit sporulation prior to aggregation.

Δ*cheY7* strain, while residues in the α4-β5-α5 fold, including G86, T104, P106, and F107, are essential for interaction with Cpc7. Residues corresponding to those positions in *E. coli* CheY are required for proper interaction with CheZ. Furthermore, the predicted structure of CheY7 places F107 within the linker region between β5 and α5 and facing the cleft created by the α4-β5-α5 fold (Fig. 3C). Replacement of residue F107 with alanine abolished CheY7's ability to complement the Δ*cheY7* cells for aggregation, indicating that this region is required for function. Therefore, the results indicate that CheY7 acts like a typical REC domain yet interacts with a previously unknown target.

HEAT repeat domains are alpha helix folds found in proteins in bacteria, archaea, and eukaryotes. Two anti-parallel alpha helices comprise each HEAT domain, and they are often found in tandem repeats, creating large, solenoid structures (36). A model of Cpc7 threaded onto known HEAT repeat proteins using Phyre2 indicates that Cpc7 is made of 27 tandem alpha helices (45). Proteins containing HEAT repeats can vary in function and have been described as having roles in scaffolding (36), lyase function (34, 35), iron binding (37), and [Fe-S] cluster stabilization (38, 39). While the mechanism of Cpc7-mediated regulation of development in *M. xanthus* is still unknown, we predict that it is involved in production of a developmental signal. The *che7* mutant phenotypes were observed under a relatively high cell density (Fig. 2), suggesting that a density-dependent factor accumulates in the parent strain. Che7 may be involved in maintaining levels of this factor, and we are currently investigating this possibility.

Lastly, this work describes an alternative cellular function for a chemosensory system. The Che7 signal transduction system impacts the coordination between aggregation and sporulation during starvation-induced development (Fig. 8). Sporulation occurs in *che7* mutants prior to aggregation, and viable spores mature earlier in *che7* mutants than in the parent. The data suggest a model in which Che7 provides a repressive checkpoint for sporulation, possibly to ensure aggregation occurs prior to sporulation, and may be related to phenotypes previously described for the EspABC and RedABCD systems in *M. xanthus* (52–55). Together, our data support a model in which a chemosensory system with a

prototypical SD-RR output regulates starvation induced development through interaction with a HEAT repeat protein.

ACKNOWLEDGMENTS

Support for this work was provided by NSF MCB-1244021 to J.R.K. Additional support for C.L.D. was provided by the Center for Biocatalysis and Bioprocessing. Start-up funds to E.J.F. were provided by the Carver College of Medicine and the Department of Biochemistry.

We thank Dan Kearns for the gift of BTH101 and David Weiss for the gift of pUT18c and pKT25 and the reviewers for critical reading of the manuscript.

The content is the responsibility of the authors and does not represent the official views of the NSF. The funding agencies had no role in study design, data collection and analysis, decision to publish, or preparation of the manuscript.

REFERENCES

1. **Sourjik V, Wingreen NS.** 2012. Responding to chemical gradients: bacterial chemotaxis. Curr. Opin. Cell Biol. **24:**262–268. http://dx.doi.org/10.1016/j.ceb.2011.11.008.
2. **Bourret RB, Borkovich KA, Simon MI.** 1991. Signal transduction pathways involving protein phosphorylation in prokaryotes. Annu. Rev. Biochem. **60:**401–441. http://dx.doi.org/10.1146/annurev.bi.60.070191.002153.
3. **Kirby JR.** 2009. Chemotaxis-like regulatory systems: unique roles in diverse bacteria. Annu. Rev. Microbiol. **63:**45–59. http://dx.doi.org/10.1146/annurev.micro.091208.073221.
4. **Güvener ZT, Harwood CS.** 2007. Subcellular location characteristics of the Pseudomonas aeruginosa GGDEF protein, WspR, indicate that it produces cyclic-di-GMP in response to growth on surfaces. Mol. Microbiol. **66:**1459–1473. http://dx.doi.org/10.1111/j.1365-2958.2007.06008.x.
5. **Hickman JW, Tifrea DF, Harwood CS.** 2005. A chemosensory system that regulates biofilm formation through modulation of cyclic diguanylate levels. Proc. Natl. Acad. Sci. U. S. A. **102:**14422–14427. http://dx.doi.org/10.1073/pnas.0507170102.
6. **Huangyutitham V, Güvener ZT, Harwood CS.** 2013. Subcellular clustering of the phosphorylated wspr response regulator protein stimulates its diguanylate cyclase activity. mBio **4**(3):e00242–13. http://dx.doi.org/10.1128/mBio.00242-13.
7. **O'Connor JR, Kuwada NJ, Huangyutitham V, Wiggins PA, Harwood CS.** 2012. Surface sensing and lateral subcellular localization of WspA, the receptor in a chemosensory-like system leading to c-di-GMP production. Mol. Microbiol. **86:**720–729. http://dx.doi.org/10.1111/mmi.12013.
8. **Berleman JE, Bauer CE.** 2005. Involvement of a Che-like signal transduction cascade in regulating cyst cell development in Rhodospirillum centenum. Mol. Microbiol. **56:**1457–1466. http://dx.doi.org/10.1111/j.1365-2958.2005.04646.x.
9. **Kirby JR, Zusman DR.** 2003. Chemosensory regulation of developmental gene expression in Myxococcus xanthus. Proc. Natl. Acad. Sci. U. S. A. **100:**2008–2013. http://dx.doi.org/10.1073/pnas.0330944100.
10. **Willett JW, Kirby JR.** 2011. CrdS and CrdA comprise a two-component system that is cooperatively regulated by the Che3 chemosensory system in Myxococcus xanthus. mBio **2**(4):e00110–11. http://dx.doi.org/10.1128/mBio.00110-11.
11. **Bren A, Eisenbach M.** 1998. The N terminus of the flagellar switch protein, FliM, is the binding domain for the chemotactic response regulator, CheY. J. Mol. Biol. **278:**507–514. http://dx.doi.org/10.1006/jmbi.1998.1730.
12. **Sarkar MK, Paul K, Blair D.** 2010. Chemotaxis signaling protein CheY binds to the rotor protein FliN to control the direction of flagellar rotation in Escherichia coli. Proc. Natl. Acad. Sci. U. S. A. **107:**9370–9375. http://dx.doi.org/10.1073/pnas.1000935107.
13. **Baker MD, Wolanin PM, Stock JB.** 2006. Signal transduction in bacterial chemotaxis. Bioessays **28:**9–22. http://dx.doi.org/10.1002/bies.20343.
14. **Welch M, Oosawa K, Aizawa S, Eisenbach M.** 1993. Phosphorylation-dependent binding of a signal molecule to the flagellar switch of bacteria. Proc. Natl. Acad. Sci. U. S. A. **90:**8787–8791. http://dx.doi.org/10.1073/pnas.90.19.8787.
15. **Ulrich LE, Zhulin IB.** 2010. The MiST2 database: a comprehensive genomics resource on microbial signal transduction. Nucleic Acids Res. **38:**D401–D407. http://dx.doi.org/10.1093/nar/gkp940.
16. **Müller S, Willett JW, Bahr SM, Darnell CL, Hummels KR, Dong CK, Vlamakis HC, Kirby JR.** 2013. Draft genome sequence of Myxococcus xanthus wild-type strain DZ2, a model organism for predation and development. Genome Announc. **1**(3):e00217–13. http://dx.doi.org/10.1128/genomeA.00217-13.
17. **Berleman JE, Scott J, Chumley T, Kirby JR.** 2008. Predataxis behavior in Myxococcus xanthus. Proc. Natl. Acad. Sci. U. S. A. **105:**17127–17132. http://dx.doi.org/10.1073/pnas.0804387105.
18. **Kroos L.** 2007. The Bacillus and Myxococcus developmental networks and their transcriptional regulators. Annu. Rev. Genet. **41:**13–39. http://dx.doi.org/10.1146/annurev.genet.41.110306.130400.
19. **Bretscher AP, Kaiser D.** 1978. Nutrition of Myxococcus xanthus, a fruiting myxobacterium. J. Bacteriol. **133:**763–768.
20. **Julien B, Kaiser AD, Garza A.** 2000. Spatial control of cell differentiation in Myxococcus xanthus. Proc. Natl. Acad. Sci. U. S. A. **97:**9098–9103. http://dx.doi.org/10.1073/pnas.97.16.9098.
21. **Magrini V, Creighton C, Youderian P.** 1999. Site-specific recombination of temperate Myxococcus xanthus phage Mx8: genetic elements required for integration. J. Bacteriol. **181:**4050–4061.
22. **Berleman JE, Kirby JR.** 2007. Multicellular development in Myxococcus xanthus is stimulated by predator-prey interactions. J. Bacteriol. **189:**5675–5682. http://dx.doi.org/10.1128/JB.00544-07.
23. **Willett JW, Tiwari N, Muller S, Hummels KR, Houtman JC, Fuentes EJ, Kirby JR.** 2013. Specificity residues determine binding affinity for two-component signal transduction systems. mBio **4**(6):e00420–13. http://dx.doi.org/10.1128/mBio.00420-13.
24. **Willett JW, Kirby JR.** 2012. Genetic and biochemical dissection of a HisKA domain identifies residues required exclusively for kinase and phosphatase activities. PLoS Genet. **8:**e1003084. http://dx.doi.org/10.1371/journal.pgen.1003084.
25. **Mauriello EM, Astling DP, Sliusarenko O, Zusman DR.** 2009. Localization of a bacterial cytoplasmic receptor is dynamic and changes with cell-cell contacts. Proc. Natl. Acad. Sci. U. S. A. **106:**4852–4857. http://dx.doi.org/10.1073/pnas.0810583106.
26. **McBride MJ, Weinberg RA, Zusman DR.** 1989. "Frizzy" aggregation genes of the gliding bacterium Myxococcus xanthus show sequence similarities to the chemotaxis genes of enteric bacteria. Proc. Natl. Acad. Sci. U. S. A. **86:**424–428. http://dx.doi.org/10.1073/pnas.86.2.424.
27. **Sun H, Zusman DR, Shi W.** 2000. Type IV pilus of Myxococcus xanthus is a motility apparatus controlled by the frz chemosensory system. Curr. Biol. **10:**1143–1146. http://dx.doi.org/10.1016/S0960-9822(00)00705-3.
28. **Black WP, Xu Q, Yang Z.** 2006. Type IV pili function upstream of the Dif chemotaxis pathway in Myxococcus xanthus EPS regulation. Mol. Microbiol. **61:**447–456. http://dx.doi.org/10.1111/j.1365-2958.2006.05230.x.
29. **Yang Z, Geng Y, Xu D, Kaplan HB, Shi W.** 1998. A new set of chemotaxis homologues is essential for Myxococcus xanthus social motility. Mol. Microbiol. **30:**1123–1130. http://dx.doi.org/10.1046/j.1365-2958.1998.01160.x.
30. **Vlamakis HC, Kirby JR, Zusman DR.** 2004. The Che4 pathway of Myxococcus xanthus regulates type IV pilus-mediated motility. Mol. Microbiol. **52:**1799–1811. http://dx.doi.org/10.1111/j.1365-2958.2004.04098.x.
31. **Kirby JR, Berleman JE, Muller S, Li D, Scott J, Wilson J.** 2008. Chemosensory signal transduction systems in *Myxococcus xanthus*, p 135–147. *In* Whitworth DE (ed), Myxobacteria: multicellularity and differentiation. ASM Press, Washington, DC.
32. **Moine A, Agrebi R, Espinosa L, Kirby JR, Zusman DR, Mignot T, Mauriello EM.** 2014. Functional organization of a multimodular bacterial chemosensory apparatus. PLoS Genet. **10:**e1004164. http://dx.doi.org/10.1371/journal.pgen.1004164.
33. **Wuichet K, Zhulin IB.** 2010. Origins and diversification of a complex signal transduction system in prokaryotes. Sci. Signal. **3:**ra50. http://dx.doi.org/10.1126/scisignal.2000724.
34. **Zhou J, Gasparich GE, Stirewalt VL, de Lorimier R, Bryant DA.** 1992. The cpcE and cpcF genes of Synechococcus sp. PCC 7002. Construction and phenotypic characterization of interposon mutants. J. Biol. Chem. **267:**16138–16145.
35. **Fairchild CD, Zhao J, Zhou J, Colson SE, Bryant DA, Glazer AN.** 1992. Phycocyanin alpha-subunit phycocyanobilin lyase. Proc. Natl. Acad. Sci. U. S. A. **89:**7017–7021. http://dx.doi.org/10.1073/pnas.89.15.7017.
36. **Kobe B, Gleichmann T, Horne J, Jennings IG, Scotney PD, Teh T.** 1999. Turn up the HEAT. Structure **7:**R91–R97. http://dx.doi.org/10.1016/S0969-2126(99)80060-4.
37. **Kim YS, Kang KR, Wolff EC, Bell JK, McPhie P, Park MH.** 2006. Deoxyhypusine hydroxylase is an Fe(II)-dependent, HEAT-repeat enzyme. Identification of amino acid residues critical for Fe(II) binding and

catalysis. J. Biol. Chem. **281:**13217–13225. http://dx.doi.org/10.1074/jbc.M601081200.
38. **Morimoto K, Sato S, Tabata S, Nakai M.** 2003. A HEAT-repeats containing protein, IaiH, stabilizes the iron-sulfur cluster bound to the cyanobacterial IscA homologue, IscA2. J. Biochem. **134:**211–217. http://dx.doi.org/10.1093/jb/mvg131.
39. **Morimoto K, Nishio K, Nakai M.** 2002. Identification of a novel prokaryotic HEAT-repeats-containing protein which interacts with a cyanobacterial IscA homolog. FEBS Lett. **519:**123–127. http://dx.doi.org/10.1016/S0014-5793(02)02736-9.
40. **Schlesner M, Miller A, Streif S, Staudinger WF, Muller J, Scheffer B, Siedler F, Oesterhelt D.** 2009. Identification of Archaea-specific chemotaxis proteins which interact with the flagellar apparatus. BMC Microbiol. **9:**56. http://dx.doi.org/10.1186/1471-2180-9-56.
41. **Kim SK, Kaiser D, Kuspa A.** 1992. Control of cell density and pattern by intercellular signaling in Myxococcus development. Annu. Rev. Microbiol. **46:**117–139. http://dx.doi.org/10.1146/annurev.mi.46.100192.001001.
42. **Birck C, Mourey L, Gouet P, Fabry B, Schumacher J, Rousseau P, Kahn D, Samama JP.** 1999. Conformational changes induced by phosphorylation of the FixJ receiver domain. Structure **7:**1505–1515. http://dx.doi.org/10.1016/S0969-2126(00)88341-0.
43. **Cho HS, Lee S-Y, Yan D, Pan X, Parkinson JS, Kustu S, Wemmer DE, Pelton JG.** 2000. NMR structure of activated CheY. J. Mol. Biol. **297:**543–551. http://dx.doi.org/10.1006/jmbi.2000.3595.
44. **Lewis RJ, Brannigan JA, Muchová K, Barák I, Wilkinson AJ.** 1999. Phosphorylated aspartate in the structure of a response regulator protein. J. Mol. Biol. **294:**9–15. http://dx.doi.org/10.1006/jmbi.1999.3261.
45. **Kelley LA, Sternberg MJ.** 2009. Protein structure prediction on the Web: a case study using the Phyre server. Nat. Protoc. **4:**363–371. http://dx.doi.org/10.1038/nprot.2009.2.
46. **Wu SS, Kaiser D.** 1997. Regulation of expression of the pilA gene in Myxococcus xanthus. J. Bacteriol. **179:**7748–7758.
47. **Lukat GS, McCleary WR, Stock AM, Stock JB.** 1992. Phosphorylation of bacterial response regulator proteins by low molecular weight phosphodonors. Proc. Natl. Acad. Sci. U. S. A. **89:**718–722. http://dx.doi.org/10.1073/pnas.89.2.718.
48. **Karimova G, Pidoux J, Ullmann A, Ladant D.** 1998. A bacterial two-hybrid system based on a reconstituted signal transduction pathway. Proc. Natl. Acad. Sci. U. S. A. **95:**5752–5756. http://dx.doi.org/10.1073/pnas.95.10.5752.
49. **Dyer CM, Dahlquist FW.** 2006. Switched or not?: the structure of unphosphorylated CheY bound to the N terminus of FliM. J. Bacteriol. **188:**7354–7363. http://dx.doi.org/10.1128/JB.00637-06.
50. **McAdams K, Casper ES, Matthew Haas R, Santarsiero BD, Eggler AL, Mesecar A, Halkides CJ.** 2008. The structures of T87I phosphono-CheY and T87I/Y106W phosphono-CheY help to explain their binding affinities to the FliM and CheZ peptides. Arch. Biochem. Biophys. **479:**105–113. http://dx.doi.org/10.1016/j.abb.2008.08.019.
51. **Guhaniyogi J, Robinson VL, Stock AM.** 2006. Crystal structures of beryllium fluoride-free and beryllium fluoride-bound CheY in complex with the conserved C-terminal peptide of CheZ reveal dual binding modes specific to CheY conformation. J. Mol. Biol. **359:**624–645. http://dx.doi.org/10.1016/j.jmb.2006.03.050.
52. **Higgs PI, Jagadeesan S, Mann P, Zusman DR.** 2008. EspA, an orphan hybrid histidine protein kinase, regulates the timing of expression of key developmental proteins of Myxococcus xanthus. J. Bacteriol. **190:**4416–4426. http://dx.doi.org/10.1128/JB.00265-08.
53. **Lee B, Higgs PI, Zusman DR, Cho K.** 2005. EspC is involved in controlling the timing of development in Myxococcus xanthus. J. Bacteriol. **187:**5029–5031. http://dx.doi.org/10.1128/JB.187.14.5029-5031.2005.
54. **Higgs PI, Cho K, Whitworth DE, Evans LS, Zusman DR.** 2005. Four unusual two-component signal transduction homologs, RedC to RedF, are necessary for timely development in Myxococcus xanthus. J. Bacteriol. **187:**8191–8195. http://dx.doi.org/10.1128/JB.187.23.8191-8195.2005.
55. **Jagadeesan S, Mann P, Schink CW, Higgs PI.** 2009. A novel "four-component" two-component signal transduction mechanism regulates developmental progression in Myxococcus xanthus. J. Biol. Chem. **284:**21435–21445. http://dx.doi.org/10.1074/jbc.M109.033415.